Hydrology and Earth System Sciences, 4, *813–822* (1997) © EGS

Hydrology & Earth System Sciences

Preferential transport of water and ^{131}Iodide in a clay loam assessed with TDR-techniques and boundary-layer flow theory

A. Mdaghri Alaoui[1], P. Germann[1], L. Lichner[2], and V. Novak [2]

[1] Soil Science Section, Department of Geography, University of Bern, Hallerstrasse 12, CH-3012 Bern, Switzerland
[2] Institute of Hydrology, Slovak Academy of Sciences, Racianska 75, P.O. Box 94, 830 08 Bratislava, Slovakia

Abstract

Rapid soil moisture variations were measured with TDR equipment at five depths ranging from 0.1 to 0.9 m during five consecutive infiltration experiments under ponding. Each time, 27 mm of water were applied. The water of the second experiment was spiked with 200 mbq of K^{131}I-tracer. Its activity was recorded as functions of depth and time with Geiger-Müller probes in 12 vertically installed access tubes. The soil moisture variations were classified as showing (i) no reaction, (ii) monotonous increase, and (iii) rapid increase followed by a gradual decrease. Reaction type (iii) was investigated further according to the boundary-layer flow theory and diagnosed as preferential flow. Rapid variations of ^{131}I-activities occurred at all depths showing soil moisture reaction type (iii). However, some of the reaction types (i) and (ii) also included rapid variations of the activities.

The approach based on boundary-layer flow theory allows fluxes to be estimated from soil moisture variations. Seven estimated total volumes of rapid flow ranged from 0.15 to 1.1 of the applied volume of water, and in only one case was the total volume badly overestimated by a factor of almost 3. The approach is worth further exploration.

Introduction

Radioactive wastes, pesticides, and other hazardous materials in soils may threaten ground and well waters. The ability to contain, control, and treat these contaminants depends on the understanding of the physical processes involved in their release to, transport within, and interaction with the subsurface environment.

Water and solutes can move preferentially in soils containing macropores, by-passing much of the soil matrix (Thomas and Phillips, 1979; Beven and Germann, 1982; Watson and Luxmoore, 1986; Jaynes *et al.*, 1988; Butters *et al.*, 1989; Singh and Kanwar, 1991). Vertically oriented macropores can greatly increase water flow, as shown by Edwards *et al.* (1979) and Davidson (1985), and field transport phenomena may be a direct consequence of root systems. Several authors demonstrated by-pass flow by examining the depth distribution of chemical tracers (Germann *et al.*, 1984; Jury *et al*, 1986; Roth *et al.*, 1991; Ritsema *et al.*, 1993), by measuring the concentration of chemicals in tile drains (Steenhuis and Muck, 1988; Kladivko *et al.*, 1991) and by investigating flow in earthworm burrows (Edwards *et al.*, 1989, 1993), and subsurface flow (Luxmoore *et al.*, 1990). Flow paths were also highlighted with methylene blue (see, for instance, Flury *et al.*, 1994; Bouma and Decker, 1978). Van Ommen *et al.* (1988) used anionic iodide to demonstrate water sorption during infiltration. However, destructive sampling restricts dying techniques to single experiments.

Direct assessment of by-pass flow is challenging technically because of the spatial and mainly temporal variability during water movement in field soils. Thus, progress in the investigation of by-pass flow in field soils must rely on non-destructive, rapid measuring techniques and related theoretical approaches.

This study assesses flow *in situ* with minimum disturbance from rapid soil moisture measurements. Preferential flow is estimated from the soil moisture data according to Germann and DiPietro (1996). In addition, the transport of radioactive K^{131}I was studied by using an *in-situ*-analyser technique.

Soil and Methods

A) SOIL

The experiments were conducted on a black clay loam (*Chernozem*) under corn (*Zea mais*). The parent material originates from fluvial deposits from the Danube river near Bratislave, Slovakia. Textural analyses, bulk densities, ρ_b,

Table 1. Texture, bulk density, pb, and hydraulic conductivity at saturation, Ks (mean, standard deviation, SD, and coefficient of variance, CV) of the soil.

depth	particle size distribution (% by weight)				ρ_b	K_S		
	diameter classes (mm)					mean	SD	CV
	<0.002	0.002–0.05	0.05–2.0	>2.0				
m	%	%	%	%	Mg/m³	m/s	m/s	%
0–0.1	29	42	28.7	0.3	—	7.9×10^{-6}	2.3×10^{-5}	290
0.1–0.2	23	46	29.5	1.5	—	6.0×10^{-6}	1.2×10^{-5}	200
02.–0.3	24	43	32.5	0.5	1.47	6.7×10^{-7}	7.7×10^{-7}	120
0.3–0.4	17	49	33.0	1.0	1.55	4.2×10^{-6}	6.0×10^{-6}	140
0.4–0.5	21.5	46	32.4	0.1	1.37	7.0×10^{-6}	1.2×10^{-5}	170
0.5–0.6	27	39	34	0	1.41	4.0×10^{-6}	2.2×10^{-6}	60
0.6–0.7	22.7	44	33.3	0	1.39	3.4×10^{-6}	2.1×10^{-6}	60
0.7–0.8	18	50	32	0	1.37	1.7×10^{-6}	5.5×10^{-7}	30
0.8–0.9	19	59	22	0	1.38	1.6×10^{-6}	1.7×10^{-6}	100
0.9–1.0	19.6	70	10.4	0	1.39	1.6×10^{-6}	4.7×10^{-7}	30

and hydraulic conductivities at saturation, K_S, are reported in Table 1. The standard deviations, SD, and the coefficients of variance, CV (i.e., standard deviation expressed as percentage of the mean), of the 9 replicas of K_S measurements at each 0.1-m depth increment are also compiled.

Organic matter was about 4% by weight in the plough layer (i.e., to the 0.3-m depth). It was almost negligible in the lower horizons. Previous infiltration experiments and the presence of main roots to the 0.6-m depth suggested a system of flow-active macropores. This notion is supported by the CVs of K_S which exceed 100% between the soil surface and 0.5-m depth but are considerably smaller below that depth (with the unexplicable exception of the horizon between 0.8 and 0.9 m). The corn stalks were cut prior to the experiments.

B) FIELD METHODS

Volumetric soil moisture θ m^3/m^{-3} was measured with a TDR-system. A wave-guide consisted of a pair of rods of stainless steel, 50 mm apart, with diameters and lengths of 6 mm and 0.3 m, respectively. An RF-Pulse transformer (500 kHz to 1 GHz and 50 to 200 Ω) was used to stabilize the signal on the Tektronix 1502B cabletester. The wave guides were multiplexed with a SDMX50 50W Coax Multiplexer, which was controlled by a 21X Campbell Micrologger. The TDR-system was calibrated according to Roth *et al.* (1990) who separated the impact of the wave-guide geometry from the soil properties, such as bulk density and the contents of clay and organic matter, on the dielectric constant. The limit of significant differences among individual measurements with the same wave guide was assessed at 0.002 m^3/m^3. Five TDR-wave guides were inserted horizontally into the soil profile at depths of 0.1, 0.3, 0.5, 0.7, and 0.9 m underneath the infiltration area, as shown in Fig. 1. The time steps of recording were set to 300 s.

Five infiltration experiments, subsequently labelled run 1 to run 5, were performed under ponding conditions by periodically and gently sprinkling 27 mm of water on the soil surface into the confined area of 1×1 m. Water was applied manually with a watering can in small amounts such that ponding was maintained during infiltration and that its depth did not exceed a few millimeters. The time to infiltrate 27 mm varied among the five runs according to the actual infiltrability of the soil surface as listed in Table 2.

Table 2. Times, durations, and average rates $\overline{q}_s$ of the five infiltration runs.

run	date	beginning time h	infiltration	duration s	$\overline{q}_s$
t_1	20.7.95	16.13	water	1630	$1.65\ 10^{-5}$
t_2	21.7.95	10.30	**Iodide**	4800	$5.63\ 10^{-6}$
t_3	22.7.95	9.46	water	7440	$3.63\ 10^{-6}$
t_4	23.7.95	9.35	water	10500	$2.57\ 10^{-6}$
t_5	24.7.95	9.35	water	9300	$2.90\ 10^{-6}$

Radioactive potassium iodide, $K^{131}I$, with a half-life of 8.09 days and an original activity of 200 mbq, was added to the water of run 2. Translocation of ^{131}I was followed by three Geiger-Müller (GM-) probes with diameters of 6.3 mm and lengths of 21 mm. The analogue interface of each probe was connected with a coaxial cable to a nuclear

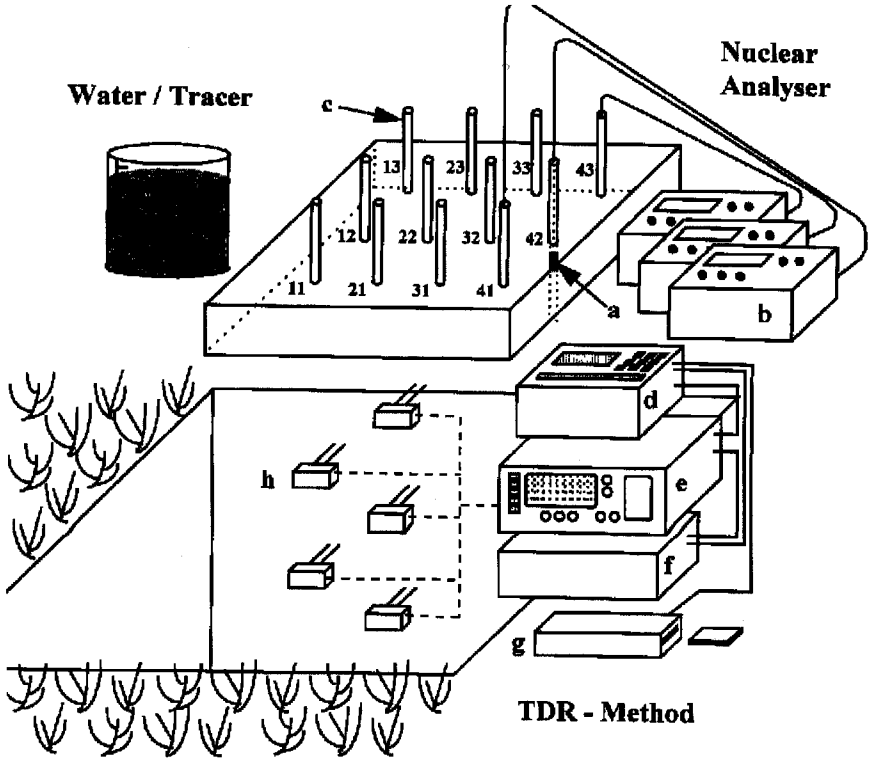

Fig. 1. *Instrumentation of the soil block. (a) Geiger-Müller probe; (b) nuclear analyser; (c) access tubes for Geiger-Müller probes; (d) data logger; (e) cable tester; (f) multiplexer; (g) card storage module; (h) TDR wave guides.*

analyser (Lichner, 1985). The probes were alternatively inserted into twelve duralium access tubes with inner and outer diameters of 8 and 12 mm, respectively, reaching to a depth of 1m. Radioactivity was measured periodically in depth increments of 0.1 m , as it is shown in Fig. 1. The data were corrected for radioactive decay. The limit of significant differences among single measurements was assessed at 20 counts per second (cps).

C) LABORATORY INVESTIGATION:

ρ_b and K_S were determined from undisturbed cylinder samples with a diameter of 53 mm and a height of 45 mm. Nine replicas were taken from each layer of 0.1 m thickness. The samples were taken between the access tubes of the G-M-probes (Fig. 1). The results are reported in Table 1. Soil texture was determined from grab samples collected at the corresponding depth increments.

Results

MOISTURE MEASUREMENTS

The soil moisture readings are shown on the left hand side of Fig.2. The five vertical lines, marked from t_1 to t_5, represent the beginning of infiltration of the respective run.

Prior to the first infiltration experiment soil moisture, $\theta_{0,1}$ m^3/m^3, throughout the profile was in the low range of $0.3 \leq \theta_{0,1} < 0.36$ m^3/m^3; this also indicated low initial capillary potentials. Temporal soil moisture variations reflect three types of reactions to infiltration:

(i) No immediate increase with barely significant, and apparently periodic, fluctuations, as illustrated at the depths of 0.3 to 0.9 m, runs 1 and 2; at the depths of 0.7 and 0.9 m, runs 3 and 4.

(ii) Monotonous increase without immediate decrease, as demonstrated at the depth of 0.1 m, run 1; at the depths of 0.3 and 0.5 m, run 3; and at the depths of 0.7 and 0.9 m , run 5.

(iii) Rapid increase during infiltration, followed by a gradual decrease shortly after the cessation of infiltration, as shown at the depth of 0.1 m, runs 2 to 5 and at the depths of 0.3 and 0.5 m, runs 4 and 5.

RADIOACTIVITY MEASUREMENTS

Only the data from two access tubes, numbers 21 and 31, are presented graphically here due to their vicinity to the TDR-wave guides, and only data from comparable depths are summarized on the right hand side of Fig. 2. The averages and CVs of the 12 activities within a horizon,

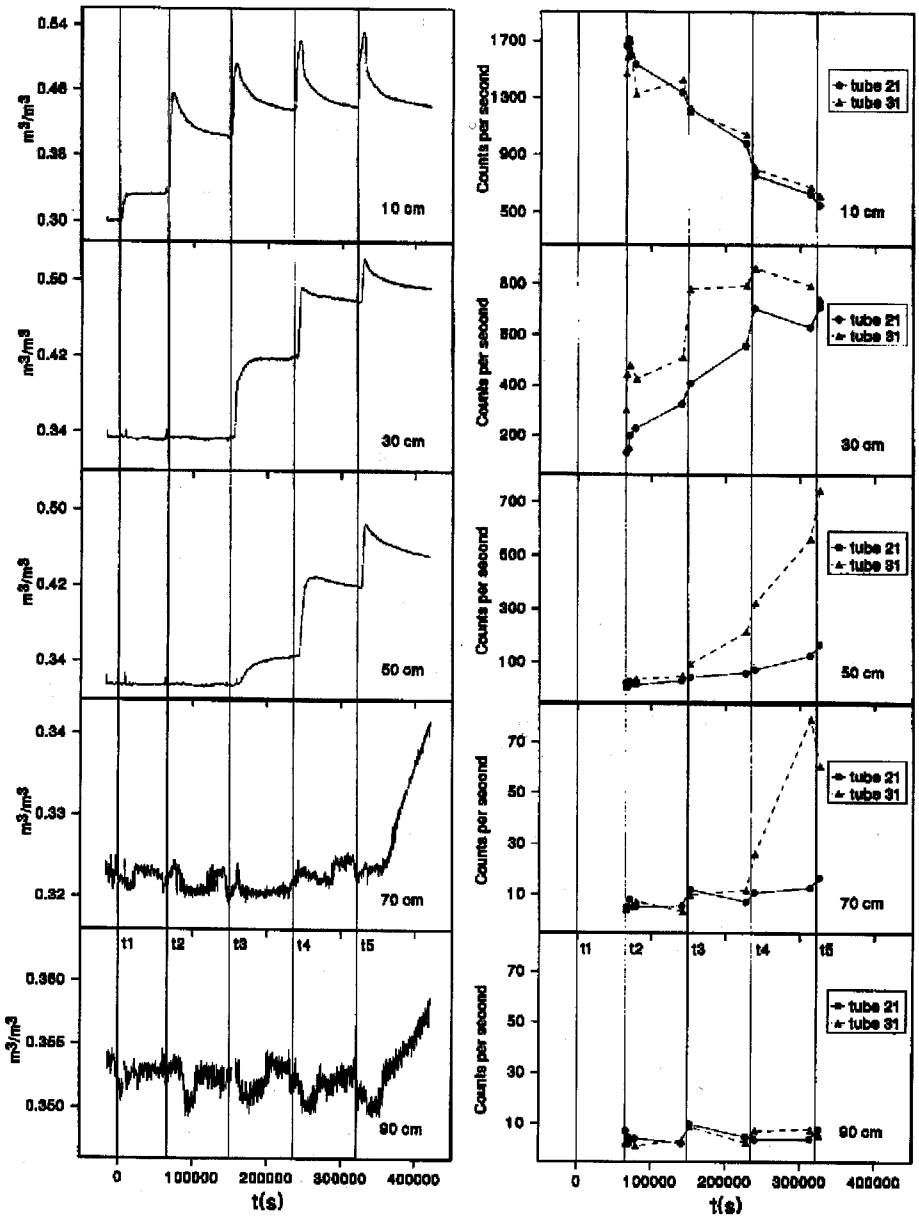

Fig. 2. *Temporal variations of soil moisture θ m^3/m^3, and activity cps of ^{131}I in access tubes 21 and 31 at depths 0.1, 0.3, 0.5, 0.7, and 0.9 m. The vertical lines, marked with t_1 to t_5, indicate the beginning of the corresponding infiltration run.*

measured approximately one hour before and two hours after infiltration, are compiled in Tab. 3 for runs 3, 4, and 5 and depths 0.1, 0.3, and 0.5 m. Reductions of CVs from before to after infiltration were observed in seven out of the nine cases, whereas the CVs of ^{131}I-activities increased during run 4 at depths 0.1 and 0.5 m. However, F-tests at the 0.95-level revealed that the variances among the 12 ^{131}I-activities did not change significantly from before to shortly after infiltration.

Discussion

A) VARIATIONS OF SOIL MOISTURE

The sequences followed by the reaction types of soil moisture variations were always from (i) → (ii) → (iii) with respect to depth and time (i.e., from the upper left to the lower right corner of the left hand side of Fig. 2), and no reverse development was observed.

Strictly speaking, type (i) indicates steady flow at the

Table 3. Mean activities (counts per second, cps) and their coefficients of variance, CV (%), of ^{131}I before and after infiltration.

Run	time relative to infiltration	at depth 0.1 m		0.3 m		0.5 m	
		mean cps	CV %	mean cps	CV %	mean cps	CV %
3	1 hour before	1023	33	340	66	72	136
	2 hours after	1086	25	439	64	85	121
4	1 hour before	992	18	543	46	130	84
	2 hours after	904	22	634	43	117	87
5	1 hour before	814	19	629	41	271	72
	2 hours after	722	18	666	38	328	70

corresponding depth; however, it is reasonable to assume that no flow has arrived at it. At the present time, there is no explanation of the seeming periodicities of soil moisture, as they appear at depths 0.7 and 0.9 m, particularly well visible due to the effect of scale enhancement. Temperature effects are ruled out because no relation with the time of the day could be found although the weather was dry and warm during the entire period of the experiments.

Type (ii) indicates pronounced consumption of flow-driving energy due to the diffusion of capillary potential, as follows from the Richards (1931)-Equation and as argued by Germann *et al.* (1997). Here, this type of energy consumption is not discussed further.

Type (iii) deserves attention because the decreasing limb of soil moisture may indicate substantial dissipation of momentum due to viscosity. Germann *et al.* (1997) argued that momentum dissipation might be significant whenever soil moisture diffusivity, D (according to the Richards-Equation) exceeds the kinematic viscosity of water, η (both [L^2 T^{-1}]). The theory of laminar boundary-layer flow deals explicitly with momentum dissipation due to viscosity, and the theory of kinematic waves provides the mathematical tool to apply it to flow in soils. Accordingly, the wetting and draining fronts of an input pulse constitute moving shock boundaries which are dealt with by the method of characteristics (Germann and DiPietro, 1996). However, not all type (iii) behaviours are *a priori* due to dominant momentum dissipation, and a more detailed analysis is required.

Newton's law of shear leads to the theory of laminar boundary-layer flow, from which Beven and Germann (1981) and Germann (1990), among others, derived the general flux law of of a kinematic wave as

$$q = bw^a \qquad (1)$$

where q m/s is the volume flux density, b m/s is the conductance parameter, w m^3/m^3 is the mobile soil moisture participating in the flow process, and a is a dimensionless exponent. (Note: Generally $w << \theta$). Based on detailed geometrical reasons, Germann and DiPietro (1996) classified drainage flow with the help of exponent a:

$2 \le a \le 3$ Laminar boundary-layer flow (within cylinders, along planes)
$3 \le a \le\approx 8$ Preferential flow in soils
$a >\approx 8$ Flow according to the Richards (1931)-Equation

The pronounced correlation between local specific momentum of flow, $\langle i \rangle$ kg/(m.s), and the exponent a, as found by Germann *et al.*(1997), supports the classification scheme strongly. For a specific soil, they arrived at $\log\langle i(a)\rangle = -1.77a + 2.44$, with a coefficient of determination of $r^2 = 0.91$ and 5 degrees of freedom. In their particular example, an increase of a from 3 to 8 decreased specific momentum $\langle i(8)\rangle/\langle i(3)\rangle$ to about 1.4×10^{-9}.

The theory of kinematic waves is here briefly reviewed to the point of intepreting type (iii)-soil moisture variations. The water input to the soil surface is considered as a rectangular pulse of volume flux density q_s [L T^{-1}] and duration t_s [T], resulting in the initial and boundary conditions of

$$t \le 0 \text{ and } t \ge t: \quad q(0,t) = w(0,t) = 0 \qquad 2(a)$$

$$0 \le t \le t_s: \quad q(0,t) = q_s; \quad w(0,t) = w_s = \left(\frac{q_s}{b}\right)^{1/a} \qquad 2(b)$$

$$0 \le z \le \infty: \quad q(z,0) = w(z,0) = 0 \qquad 2(c)$$

The temporal variation of soil moisture at depth $Z \le z_I = t_S \dfrac{abw^{a-1}}{(a-1)}$ is

$$a \ge t \ge t_w \qquad w(Z,t) = 0 \qquad 3(a)$$

$$t_W(Z) \le t \le t_D(Z) \qquad w(Z,t) = w_S \qquad 3(b)$$

$$t \ge t_D(Z): \qquad w(Z,t) = w_{S,Z}\left(\frac{t_D(Z) - t_s}{t - t_S}\right)^{\frac{1}{(a-1)}} \qquad 3(c)$$

$$t_W(Z) = \frac{Z}{b w_{S,Z}^{(a-1)}} \qquad 3(d)$$

$$t_D(Z) = t_s + \frac{Z}{ab w_{S,Z}^{(a-1)}} \qquad 3(e)$$

where $t_W(Z)$ and $t_D(Z)$ are the arrival times of the wetting and draining shock fronts at depth Z, respectively, and z_I is the depth at which the draining front intercepts the wetting front i.e, henceforth $q(Z \geq z_I, t)$ and $w(Z \geq z_I, t)$ are single-crested functions of time. For details see Germann and DiPietro (1996). The solid line in Fig. 3 illustrates a complete kinematic wave according to Eqns (3a) to (e).

The procedure to estimate the parameters $w_{s,z}(t_w < t < t_D)$, a, and b of the kinematic wave model from data $w(Z,t_i) = \theta(Z)_{max} - \theta(Z,t_i)$ at depth Z follows three steps. Firstly,

$$w_{S,Z}(t_W < t < t_D) = \theta(Z)_{max} - \theta(Z)_E, \qquad (4a)$$

where $\theta(Z)_{max}$ is the maximum soil moisture content, and $\theta(Z)_E$ is the moisture content remaining at depth Z after the passing of the kinematic wave as it is illustrated in Fig. 3. Secondly, the exponent a and the arrival time of the draining front at depth Z, $t_D(Z)$, are determined from a linear regression analysis $Y_i = AX_i + B$. Equation (3c) yields

$$\ln\left(\frac{w(Z,t_i)}{w_S(Z)}\right) = \frac{1}{a-1}\ln\left(\frac{t_D(Z) - t_S}{t_i - t_S}\right). \qquad (4b)$$

where $Y_i = \ln(w(Z,t_i)/w_{s,z})$, $X_i = \ln((t_D(Z) - t_s)/(t_i - t_s))$, and $A = 1/(a-1)$. The time $t_D(Z)$ in Eqn.(4b) is optimized by trial and error such that the coefficient of determination, $r^2 \rightarrow 1.0$ and $B \rightarrow 0$. Further,

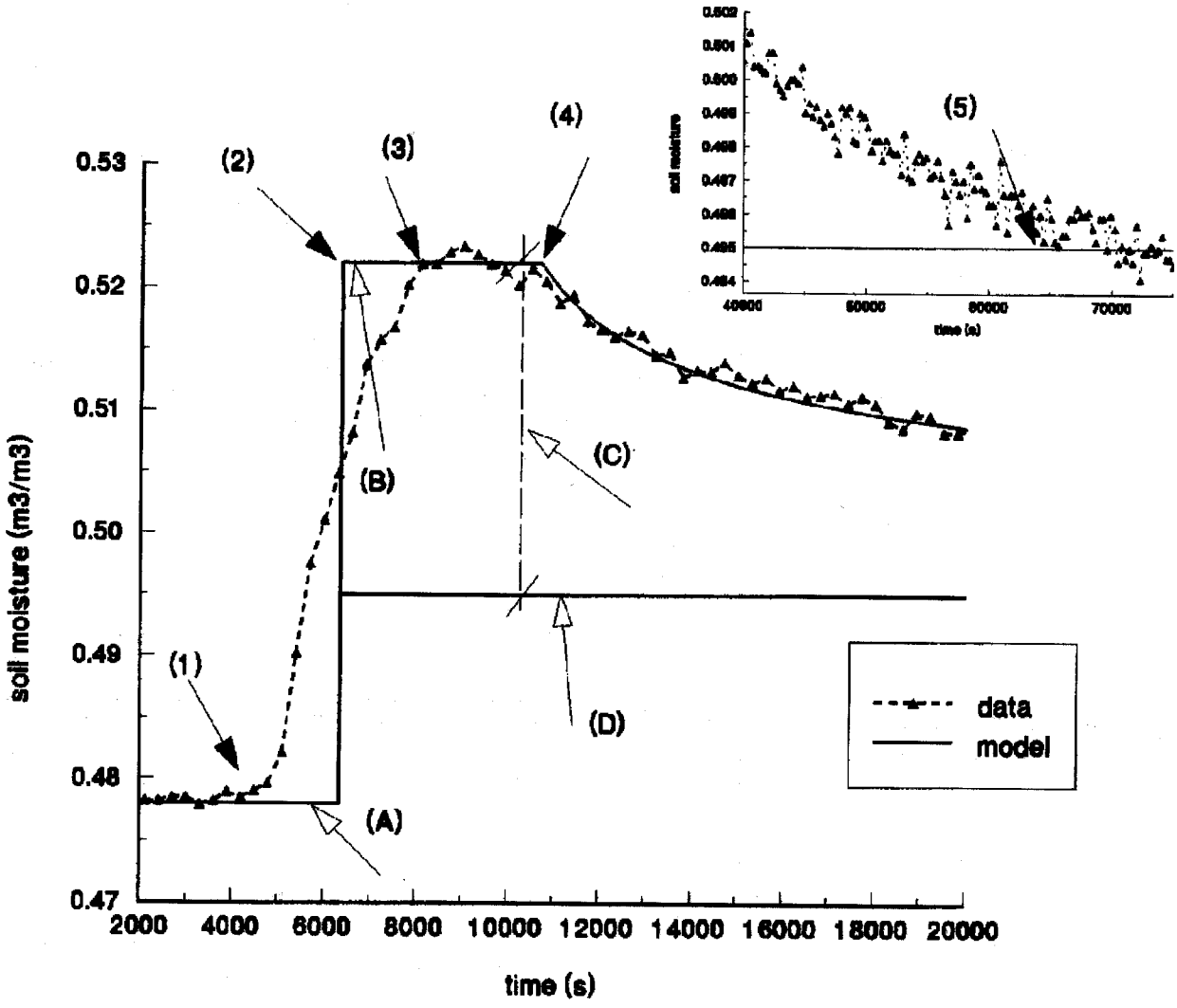

Fig. 3. *Measured and modelled soil moisture variations $\theta(Z,t)$, run 5 at the 0.3-m depths. (1) and (3) observed first and last arrival times of the wetting front; (2) modelled arrival time of the wetting front, $t_w(Z)$; (4) arrival time of the draining front, $t_D(Z)$ (observed and used in the model); (5) final soil moisture, θ_E. (A) initial soil moisture, θ_0; (B) maximum soil moisture, θ_{max}; (C) difference between maximum and final soil moisture, $w_{s,z}$, which has passed the 0.3-m depth as kinematic wave; (D) assumed dividing line between soil moisture sorbed by capillarity, $\theta_E - \theta_0$, and $w_{s,z}$.*

Table 4. Model parameters a, b, $w_{s,z}$, and $t_w(Z)$, the coefficient of determination, r^2, between measured and modelled soil moisture for $t > t_D(Z)$, and estimated total volume of macropore flow, $V(Z)$ mm, which has passed the depth Z of measurement during the respective infiltration run.

Z m	run	a —	b m/s	$w_{s,z}$ m³/m³	$t_w(Z)$ s	$t_D(Z)$ s	r^2 —	$V(Z)$ mm	$V(Z)/V(0)$ —
0.1	2	3.7	0.048	0.050	6040	9350	0.94	6.4	0.24
	3	3.2	0.006	0.052	7440	9515	0.99	4.0	0.15
	4	3.1	0.012	0.081	1557	11005	0.91	79.6	2.95
	5	3.3	0.008	0.090	2828	10164	0.99	29.6	1.10
0.3	4	4.0	23.4	0.013	6796	12180	0.88	6.1	0.23
	5	3.8	1.270	0.027	6352	10685	0.86	12.5	0.46
0.5	4	4.2	81.3	0.009	19150	35580	0.85	7.4	0.27
	5	3.0	0.048	0.032	10490	12780	0.95	14.3	0.53

$$a = \frac{1-A}{A}.$$

Thirdly, from Eqn. (3e) it follows that

$$b = \frac{(t_D(Z) - t_S)}{a w_{S,Z}^{(a-1)}}$$

The results of the analyses are compiled in Tab. 4
All eight sequences of type (iii)-θ-variations demonstrate preferential flow according to the kinematic wave model with $3 \le a \le 4.2$ and $0.009 \le w_{s,z} \le 0.09$.

The arrival time of the wetting front at depth Z, $t_w(Z)$, can be estimated by inserting the model parameters into Eqn. (3d). The model performance can be validated by comparing the estimated arrival times, $t_w(Z)$, with those observed t_{w1} and t_{w2} (Fig 3) because the modelled arrival times of the wetting front $t_w(Z)$ were calculated solely from $\theta(Z, t \ge t_D)$. Two observed arrival times of the wetting fronts, t_{w1} and t_{w2}, are reported here due to their spreading, as shown in Fig. 3. The fact that estimated arrival times fall between the observed arrival times i.e., $t_{w,1} \le t_w(Z) \le t_{w,2}$, at the 0.3- and 0.5-m depths (as compiled in Table 5) supports the kinematic wave approach. (For details, see Germann and DiPietro, 1996.)

The total volume of flow, $V(Z)$ m which has passed at Z as kinematic wave during $t_w(Z) \le t \le \infty$ follows from integration of Eqns (3b and c) under the consideration of Eqn. (1):

$$V(Z) = b w_{S,Z}^{a} \left(\int_{t_W(Z)}^{t_D(Z)} dt + (t_D(Z) - t_S)^{a/(a-1)} \int_{t_D(Z)}^{\infty} (t - t_S)^{-a/(a-1)} dt \right),$$

leading to :

$$V(Z) = b w_{S,Z}^{a} (a t_D(Z) - (a-1) t_S - t_W(Z)) = b w_{S,W}^{a} t_S$$

(For details see Germann *et al.*, 1997). The results of the data analyses are compiled in Table 4.

Table 5. Observed and calculated arrival times of the wetting fronts, t_{w1}, t_{w2}, and $t_w(z)$, respectively; estimated total volume of flow, $V(z)$, and ratio to the input volume, $V(0)$.

z m	run	t_{w1} s	$t_w(z)$ s	t_{w2} s	$V(z)$ mm	$V(z)/V(0)$
0.1	2	900	6040	5400	6.4	0.24
	3	1680	7440	5640	4.0	0.15
	4	1680	1557	6980	79.6	2.95
	5	780	2828	6480	29.6	1.10
0.3	4	5880	6796	9480	6.1	0.23
	5	6000	6352	8880	12.5	0.46
0.5	4	8280	19150	27000	7.4	0.27
	5	6780	10490	10980	14.3	0.53

The volumes of estimated preferential flow are within the limits of $0 < V(Z) \le V(0) = 27$ mm. The two exceptions are $V(0.1m,run4) \approx 80$ mm and $V(0.1m,run5) \approx 30$ mm or about 3 and 1.1 times the volume of water applied to the soil surface. From a technical point of view, these deviations may hint at difficulties in correctly measuring soil moisture with the TDR-method near the soil surface. Fissures which evolved in the course of experimentation may have exposed parts of the wave guide; alternatively its original close contact with the soil matrix may have loosened. The interpretation of the soil moisture data may provide another source of uncertainty. Equation (4a) requires an estimate of $\theta(Z)_E$ and assumes its being constant during the passing of the wave. The deviations of the estimates as well as the inadequacy of the assumption could be enhanced due to the relatively low infiltration rates during the two runs. However, the coefficients of determination r^2 of the linear regression between the measured and the calculated moisture contents, as reported in Tab. 4, favour other inadequacies.

The sensitivity of applying the kinematic wave approach to the data with respect to the estimation of $\theta(Z)_E$, and thus of $w_{s,z}$ (i.e., the positioning of line (*D*) in Fig. 3) is demonstrated in Tab. 6. Mobile moisture $w_{s,z} = 0.027$ was used in the original optimisation of the exponent a and the arrival time of the draining front $t_D(Z)$. It was varied within $0.047 \geq w_{s,z} \geq 0.012$ using steps of 0.005, and the corresponding opitmisations, Eqns 4(a) to (d), were repeated with the original data. The arrival times of the draining front thus varied slightly within $10640 \leq t_D(Z) \leq 10801$ s, but those of the modelled wetting fronts within $2070 \leq t_w(Z) \leq 7073$; the exponents were found within $1.51 \leq a \leq 5.1$, the conductances within $1.32\ 10^{-3} \leq b \leq 11.8$, and the ratios of the total volumes of flow within $0.55 \leq V(Z)/V(0) \leq 0.70$. Uncertainties in the estimation of $w_{s,z}$ thus affect a and b the most. The strong correlation between a and b follows from dimensional analysis. Conceptually, Germann and DiPietro(1996) found that

$$b = \frac{g}{6\eta} C^{a-1} F^{3-a} l^{1-a},$$

where C m^2 is the cross-sectional area of the soil, F m is the thickness of the water film, and l m is the perimeter of the mobile water within C. Due to integration, Eqns (5a,b), the ratios $V(Z)/V(0)$ and thus the volume flux *densites* $q_{s,z} = b w_{s,z}^a$ (Eqn. 1) remained well confined.

B) VARIATIONS OF ACTIVITIES

Significant transport of ^{131}I was observed in tube 21 to 0.5 m, and in tube 31 to 0.7 m depth. Monotonous decrease and increase of activities indicate net leaching and net accumulation, respectively, of iodide at the corresponding depth. Simultaneous opposing developments of activities indicate the spatial heterogeneity of iodide transport, as is shown at the 0.1-m depth, between t_2 and t_3, and at the 0.3-m depth, before and after t_2 and t_5. Rapid variations of activities, either increases or decreases, occurred during the eight observed flow types (iii), which were diagnosed as preferential flow according to the theory of laminar boundary-layer flow. However, similar activity variations also occurred during flow type (ii) as demonstrated during run 3 at depths of 0.3 m and, possibly, of 0.5 m. In both cases, it seems that the activities increased before the moisture content. Even more puzzling is the increase of activity at the 0.3-m depth, run 2, without showing any corresponding increase of soil moisture.

C) COMBINATION OF ASPECTS

Soil morphological features, translocation of K^{131}I-tracer, the CVs of K_S, the descriptive assessment of $\theta(Z,t)$, and the applicability of the kinematic wave model to the data concurrently indicate preferential flow in the depth range 0 to 0.5 m after antecedent soil moisture has reached a critical level of about 0.4 m^3/m^3. Soil moisture barely began to increase at the 0.7-and 0.9-m depths during runs 4 and 5. Thus, soil hydraulic considerations do not allow for the assessment of preferential flow and a related functional macropore system at the two depths. However, the CVs of K_S being less than 100% suggest their most likely absence.

The total volumes of preferential flow $V(Z)$ increased gradually with the increasing number of runs, indicating that preferential flow is more pronounced with higher antecedent soil moisture, as shown in Table 4, at depths of 0.3 and 0.5 m, between runs 4 and 5. However, no narrow threshold moisture content can be identified beyond which preferential flow occurs. By contrast, the average volume flux densities of water input to the soil surface in the range of $2.57\ 10^{-6} \leq \bar{q}_s \leq 1.65\ 10^{-5}$ m/s were always high enough to initiate and support preferential flow.

Conclusions

Soil moisture variations in a *Chernozem* near Bratislava were studied with the TDR method to the 0.9-m depth following five infiltration runs. A K^{131}I solution with an activity of 200 mbq was added to the water of the second infiltration experiment. The spread of activity was measured with three Geiger-Müller probes which were inserted sequentially into a total of 12 access tubes.

Generally, soil moisture at one depth reacted to infiltration in three consecutive ways: (i) no increase at all, (ii) monotonous increase, and (iii) monotonous increase

Table 6. Sensitivity analysis: model parameters as functions of w_s.

w_s	t_D s	t_w s	a	b m/s	r^2	$V(z)$ mm	$V(z)/V(0)$
0.012	10670	2070	1.51	1.32E–3	0.81	15.4	0.57
0.017	10801	3190	2.13	9.4E–3	0.89	14.9	0.55
0.022	10680	3256	2.36	1.65E–2	0.88	18.8	0.70
0.032	10640	5220	3.90	1.24	0.95	17.1	0.63
0.037	10688	6000	4.32	2.83	0.95	17.2	0.64
0.042	10686	6505	4.69	5.55	0.95	18.0	0.67
0.047	10688	7073	5.10	11.80	0.95	18.5	0.69

followed by a long-tailed decrease. All eight events of reaction type (iii) were assessed as preferential flow during those momentum dissipation due to viscosity dominated, according to Germann *et al.* (1997).

The temporal variations of ^{131}I-activities and the spatial variations of hydraulic conductivities support the notion of preferential flow. However, similar activity variations were diagnosed in connection with soil moisture reactions types (i) and (ii) which shows that not only preferential flow according to Germann and DiPietro (1996) led to the presumably preferred transport of iodide. Further investigations are required to assess whether preferred solute transport apparently not being associated with preferential flow is due to spatial heterogeneities of either two processes or whether flow and transport processes are involved which were not considered here.

Soil texture, bulk density and mean hydraulic conductivity are not reliable indicators of preferential flow; however, the spatial variation of hydraulic conductivity was positively related with it. Run 5, for instance, revealed that the maximum of preferential flow arrived at the 0.5-m depth about three hours after infiltration began. The minimum antecedent soil moisture content for the initiation of preferential flow was found to be about 0.4 m^3/m^3.

The application of the kinematic wave model to the data allows the total volume of water participating in preferential flow to be estimated. In seven cases, out of eight, this volume was between 15 and 110% of the volume applied to the soil surface, which is considered reasonable.

The application of radioactive tracers and TDR-technique allows for a repeated assessment of preferential flow *in situ* with a minimum of interferences with the flow system. Moreover, no impermeable layer, be it natural (i.e., leading to a water table) or artificial (i.e. drainage system, lysimeters), is required to assess preferential flow and transport in soils.

Acknowledgment

This study was funded by the Swiss National Science Foundation. Grants 7SLKAO41336 and 21–36281.92. The authors express their gratitude to Ms Vlasta Stekauerova for the tedious measurements of hydraulic conductivities and bulk densities.

References

Beven, K., and Germann, P., 1981. Water flow in soil macropores II. A combined flow model. *J. Soil Sci.* 32:15–29

Beven, K., and Germann, P., 1982. Macropores and water flow in soils. *Wat. Resour. Res.*, **18**, 1311–1325.

Bouma, J. and Dekker, L. W., 1978. A case study on infiltration into dry clay soil, l, Morphological observations. *Geoderma*, **20**, 27–40.

Butters, G. L., Jury, W. A., and Ernest, F. F., 1989. Field scale transport of bromide in an unsaturated soil. E. Experimental methodology and results. *Wat. Resour. Res.*, **25**, 1575–1581.

Davidson, M. R., 1985. Numerical calculation of saturated–unsaturated infiltration in a cracked soil. *Wat. Resour. Res.*, **21**, 709–714.

Edwards, W. M., van der Ploeg, R. R., and Ehlers, W., 1979. A numerical study of the effects of non-capillary sized pores on infiltration. *Soil. Sci. Soc. Am. J.*, **43**, 851–856.

Edwards, W. M., Shipitalo, M. J., Owens, L. B., and Norton, L. D., 1989. Water and nitrates movement in earthworm burrows within long-term not-till cornfields. *J. Soil Water Conserv.*, **44**, 240–243.

Edwards, W. M., Shipitalo, M. J., Owens, L. B., and Dick, W. A., 1993. Factors affecting preferential flow of water and atrazine through earthworm burrows under continuous no-till corn. *J. Environ. Qual.*, **22**, 453–457.

Flury, M., Flühler, H., Jury, W. A., and Leuenberger, J., 1994. Susceptibility of soils to preferential flow of water: A fields study. *Wat. Resour. Res.*, **30**, 1945–1954.

Germann, P. F., 1990. Preferential flow and the generation of runoff, 1. Boundary-layer flow theory. *Wat. Resour. Res.* **26** (12), 3055–3063.

Germann, P. F., and DiPietro, L., 1996. When is porous media flow preferential? A hydrodynamic perspective. *Geoderma* **74**, 1–21.

Germann, P. F., DiPietro, L., and Singh, V. P., 1997. Local momentum balance during flow in structured soil assessed from TDR-moisture readings. *Geoderma*, **80**, 153–168.

Germann, P. F., Edwards, W.M., and Owens, L. B., 1984. Profiles of Bromide and increased soil moisture after infiltration into soils with macropores. *Soil. Sci. Soc. Am. J.*, **48**, 237–244.

Jaynes, D. B., Bowman, R. S., and Rice, R. C., 1988. Transport of a conservative tracer in the field under continuous flood irrigation. *Soil Sci. Soc. Am. J.*, **52**, 618–624.

Jury, W. A., Elabd, H., and Resketo, M., 1986. Field study of napropamide movement through unsaturated soil. *Wat. Resour. Res.*, **22**, 749–755.

Kladivko, E. J., van Scoyoc, G. E., Monke, E. J., Oates, K. M., and Pask, W., 1991. Pesticide and nutrient movement into subsurface tile drains on a silt loam soil in Indiana. *J. Environ. Qual.*, **20**, 264–270.

Lichner, L., 1985. Modified gamma method of soil moisture velocity measurement. in: *Proc. Xth IMEKO World Congress*, **10**, Prague, pp. 92–99.

Luxmoore, R. J., Jardine, P. M., Wilson, G. V., Jones, J. R., and Zelazny, L. W., 1990. Physical and chemical controls of preferred path flow through a forested hillslope. *Geoderma*, **46**, 139–154.

Richards, L. A., 1931. Capillary conduction of liquids in porous mediums. *Physics*, **1**, 318–33.

Ritsema, C. J., Dekker, W. W., Hendrickx, J. M. H., and Hamminga, W., 1993. Preferential flow mechanism in water repellent sandy soil. *Wat. Resour. Res.*, **29**, 2183–2193.

Roth, K., Schulin, R., Flühler, H., and Attinger, W., 1990. Calibration of Time Domaine Reflectometry for water content measurement using a composite dielectric approach. *Wat. Resour. Res.*, **26**, 2267–2274.

Roth, K., Jury, W. A., Flühler, H., and Attinger, W., 1991. Transport of chloride through an unsaturated field soil. *Wat. Resour. Res.*, **27**, 2533–2541.

Singh, P. and Kanwar, R.S., 1991. Preferential solute transport through macropores in large undisturbed saturated soil columns. *J. Environ. Qual.*, **20**, 295–300.

Steenhuis, T. S. and Muck, R. E., 1988. Preferred movement of nonadsorbed chemicals on wet, shallow, sloping soils. *J. Environ. Qual.*, **17**, 376–384.

Thomas, G. W. and Phillips, R. E. 1979. Consequences of water movement in macropores. *J. Environ. Qual.* **8**, 149–152.

Van Ommen, H. C., Dekker, L. W., Dijksma, R. Hulshof, J., and van der Molen, W. H., 1988. A new technique for evaluating the presence of preferential flow paths in nonstructured soils. *Soil Sci. Soc. Am. J.*, **52**, 1192–1194.

Watson, K. W. and Luxmoore, R. J., 1986. Estimating macroporosity in a forest watershed by use of tension infiltrometer. *Soil. Sci. Soc. Am. J.*, **50**, 578–582.